BUTTERWORTH HEINEMANN

Polymer Vol. 36 No. 16, pp. 3191–3196, 1995

0032-3861/95/$10.00 + 0.00

Electrically conductive polymer fibres with mesoscopic diameters: 2. Studies of polymerization behaviour

M. Granström*, J. C. Carlberg and O. Inganäs
Laboratory of Applied Physics, Department of Physics (IFM), University of Linköping, S-581 83 Linköping, Sweden
(Received 15 August 1994; revised 6 February 1995)

Different types of conductive polymers have been synthesized within the pores of microfiltration membranes. These membranes contain linear, cylindrical pores of varying diameter from 10 nm to 10 μm. The polymerization conditions in such pores are quite different from polymerizing on a flat surface, and are therefore investigated. It is shown that the geometry for the smaller pores results in a situation where the concentration of radicals is low compared to the concentration of monomers, resulting in a material with higher conductivity. The bulk concentration of monomers is also a crucial aspect, where higher concentrations give polymer fibres with higher conductivity.

(Keywords: poly(pyrrole); polymerization conditions; conductivity)

INTRODUCTION

It has been shown a number of times that polymerizing a conductive polymer within the pores of microfiltration membranes can give the polymer a unique morphology[1] and also change the properties of the polymer, such as increasing the conductivity dramatically[2]. This behaviour has been found for different conducting polymers such as poly(pyrrole)[2,3], poly(acetylene)[4,5] and poly(3-methylthiophene)[2], and both for chemical and electrochemical polymerization. To investigate the polymerization conditions we turn to the theory of microelectrodes and arrays of these. Electrodes with small dimensions have been studied since they have some advantages compared to macroelectrodes; for example, they exhibit a much smaller potential drop, which makes it possible to measure in low concentration electrolytes, and a steady state is quickly reached without the need for convection. Their small physical size also means that they can be used where ordinary macroelectrodes are too large. One major drawback with the microelectrodes is also connected to their small physical size: the low surface area results in a small current and low signal to noise ratios[6]. To overcome these problems and maintain the advantages, the solution has been to use arrays of these microelectrodes, thereby increasing the measured current without losing too many of the advantages. To find analytical expressions for such an array, a number of situations have to be considered since the diffusion situation changes with time, starting with a number of isolated microelectrodes, reaching a state where the diffusion zones from the individual electrodes start to overlap, and ending up with a situation where all diffusion zones overlap and there is total coverage of the electrode area (both active and insulating). A transition from mainly radial diffusion to individual microelectrodes to planar diffusion to the whole plane will then occur at some specific time during the experiment (see *Figure 1*). The microelectrode array describes fairly well the situation with electropolymerization in the pores of a microfiltration membrane if it is taken into account that the microelectrodes are not only randomly distributed but also recessed. Atomic force microscopy (AFM) pictures of the surface of a membrane before and after polymerization are shown in *Figure 2*. The sample geometry and synthesis details are described in part 1 of this series.

THEORY

Each microelectrode

The geometry of the microelectrode is shown in *Figure 3*. For each such individual recessed microelectrode the current densities are given by[7]

$$j_p = \frac{4nFc^b D}{4L + \pi a} \tag{1}$$

for the steady state and

$$j_p(t) = \frac{4nFc^b D}{4L + \pi a}\theta_3\left[0, \frac{16Dt}{(4L + \pi a)^2}\right] \tag{2}$$

for the transient. The θ_3 function can be found elsewhere[8] and c^b is the bulk concentration of the reactive species. Typical experimental values for the rest of the parameters are listed in *Table 1*. The short-time and long-time expansions of the θ_3 function give the following

* To whom correspondence should be addressed

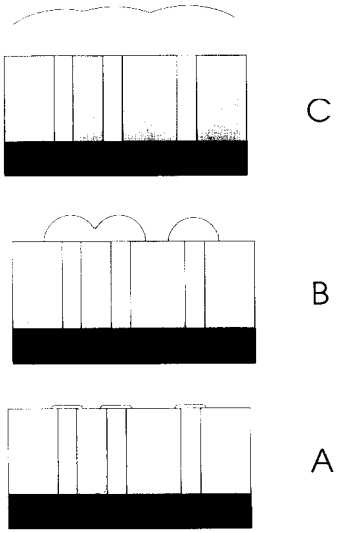

Figure 1 The diffusion zones at adjacent microelectrodes at different times ($t_a < t_b < t_c$)

Table 1 Parameter values used in the majority of the experiments

Parameter	Value
Pore radius a (nm)	50
Number of electrons n	2.25[a]
Diffusion coefficient for pyrrole D ($cm^2\ s^{-1}$)	2×10^{-5}
Depth of pore L (μm)	6
Faraday constant $F = N_A e$ ($A\ mol^{-1}$)	9.648×10^4

[a] From Diaz and Bargon[9]

approximations for the current density

$$j_p(t) = nFc^b\sqrt{\frac{D}{\pi t}}\left\{1 + 2\exp\left[-\frac{(L+\pi a/4)^2}{Dt}\right] + \cdots\right\} \quad (3)$$

for short times and

$$j_p(t) = \frac{nFc^bD}{L+\pi a/4}\left\{1 + 2\exp\left[-\frac{\pi^2 Dt}{(L+\pi a/4)^2}\right] + \cdots\right\} \quad (4)$$

for long times. Using the long-time expansion of the function, the time required to reach within a 5% deviation from the steady-state value can be calculated. The values in *Table 1* are valid for most of the conducted experiments. A 5% deviation from steady state means

$$0.05 = 2\exp\left[-\frac{\pi^2 Dt}{(L+\pi a/4)^2}\right] + \cdots \quad (5)$$

resulting in the times shown in *Table 2* for different pore sizes. This means that a very short time is needed to reach the steady-state situation and equation (1) can be used in the subsequent calculations.

Microelectrode arrays

The analytical expressions for diffusion to ensembles of microelectrodes have been extensively investigated by Scharifker[10] and a similar approach will be used here, with the addition that the microelectrodes are recessed. What makes the analysis complicated is that not only does the diffusion field from each microelectrode extend three-dimensionally, but the two-dimensional distribution of microelectrodes also makes them interact with each other. Fortunately, this three-dimensional problem can be transformed into a two-dimensional

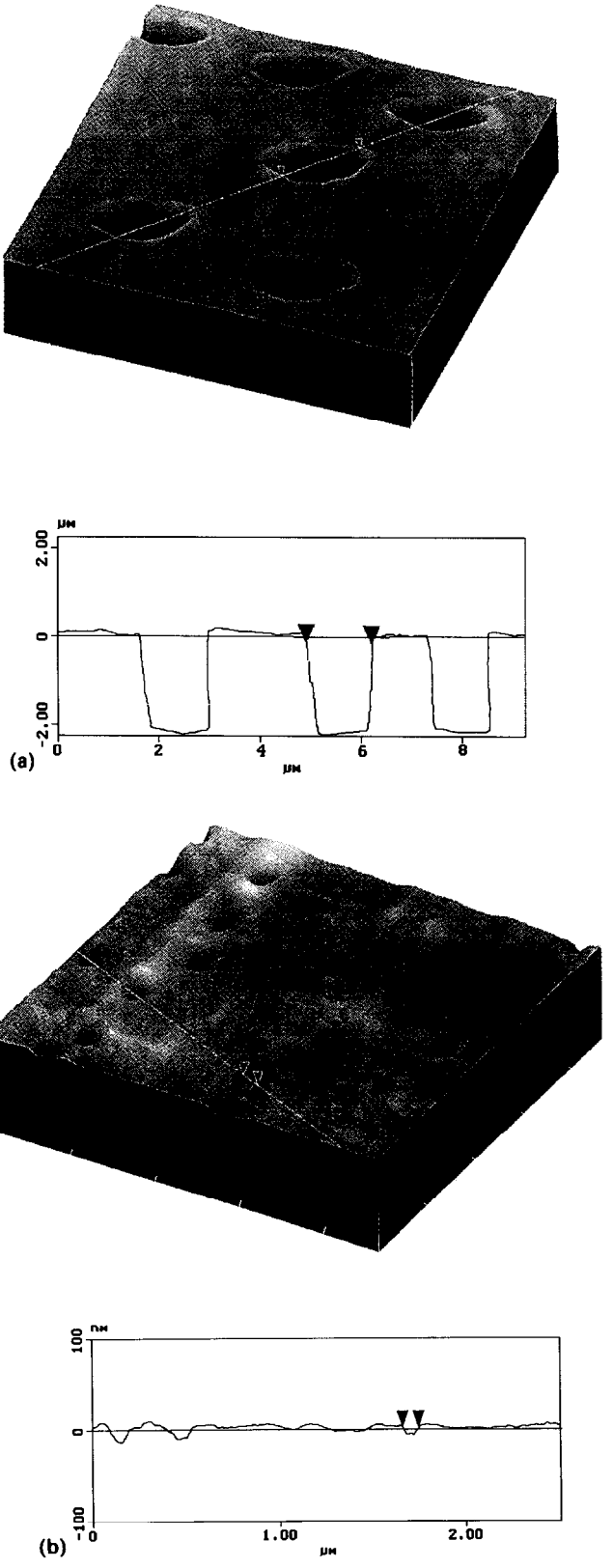

Figure 2 (a) AFM picture and section profile of an empty membrane with 1 μm pores. (b) AFM picture and section profile of a 100 nm pore membrane after polymerization

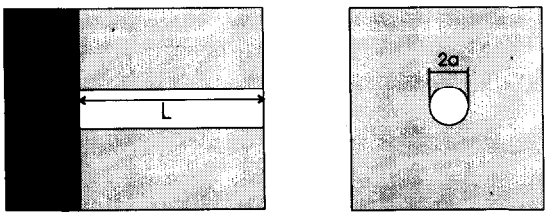

Figure 3 Microelectrode (pore) geometry

Table 2 Times needed to reach within 5% of the steady-state situation for different pore sizes

Pore radius (nm)	Membrane thickness (μm)	t (ms)
5000	10	36
500	11	24
50	6	6.8
5	6	6.7

problem[11] by defining an equivalent plane surface to which the same amount of material is transported by linear diffusion as is radially diffused to a microelectrode. For this equivalent area we must solve the diffusion equation

$$\frac{\partial c(x,t)}{\partial t} = D\frac{\partial^2 c(x,t)}{\partial x^2} \tag{6}$$

with the boundary conditions

$$c(x,0) = c^{\mathrm{b}}$$

$$\lim_{x\to\infty} c(x,t) = c^{\mathrm{b}}$$

$$c(0,t) = c^{\mathrm{m}}$$

where c^{m} is the concentration at the mouth of the pore. Assuming that c^{m} can be considered constant for a short period of time, equation (6) results in a slightly modified Cottrell equation for the current density

$$j_{\mathrm{eq}}(t) = nF(c^{\mathrm{b}} - c^{\mathrm{m}})\sqrt{\frac{D}{\pi t}} \tag{7}$$

Equating the amount of material means $\pi r_{\mathrm{d}}^2 j_{\mathrm{eq}} = \pi a^2 j_{\mathrm{p}}$, where equation (1) is used for j_{p} and r_{d} is the radius of the equivalent plane surface. The area of the plane surface can be calculated from

$$A_{\mathrm{eq}} = \pi r_{\mathrm{d}}^2 = \frac{4\pi a^2\sqrt{D\pi t}}{(4L+\pi a)}\frac{c^{\mathrm{b}}}{(c^{\mathrm{b}}-c^{\mathrm{m}})} \tag{8}$$

Random array

Since the pore densities in the membranes are below 15% and the pores are randomly distributed owing to the nuclear process with which they are initiated, the distance between pores can be estimated using the nearest-neighbour distribution. The average distance between pores is then given by[12]

$$\langle d\rangle = \frac{1}{2\sqrt{m}} \tag{9}$$

where m is the number density of the pores. The Avrami theorem[13] will then predict the statistical overlap of diffusion zones from such a distribution of point sources or microelectrodes. The fractional area covered by the diffusion zones is

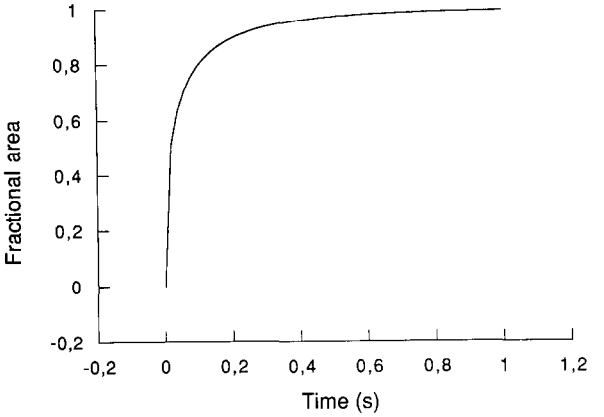

Figure 4 Plot of equation (10b) using typical experimental values

$$A = 1 - \exp\left(-\frac{A_{\mathrm{eq}}}{4\langle d\rangle^2}\right) = 1 - \exp\left(-mA_{\mathrm{eq}}\right) \tag{10a}$$

$$A = 1 - \exp\left[-\frac{4\pi m a^2\sqrt{D\pi t}}{(4L+\pi a)}\frac{c^{\mathrm{b}}}{(c^{\mathrm{b}}-c^{\mathrm{m}})}\right] \tag{10b}$$

A plot of this function with typical values from experimental conditions is given in *Figure 4*. The current density supplied to the ensemble will then be this fractional area multiplied by equation (7), resulting in

$$j = nF(c^{\mathrm{b}} - c^{\mathrm{m}})\sqrt{\frac{D}{\pi t}} \times \left\{1 - \exp\left[-\frac{4\pi m a^2\sqrt{D\pi t}}{(4L+\pi a)}\frac{c^{\mathrm{b}}}{(c^{\mathrm{b}}-c^{\mathrm{m}})}\right]\right\} \tag{11}$$

EXPERIMENTAL

Nuclepore® and Poretics® poly(carbonate) microfiltration membranes with pore diameters between 10 nm and 10 μm were used and the details of sample fabrication are described elsewhere[3]. The monomers were polymerized electrochemically using a Bioanalytical Systems BAS100A electrochemical analyser run in potentiostatic mode and a three-electrode cell with a platinum foil as the counterelectrode and Ag/AgCl as the reference electrode. To investigate the influence of salt and monomer concentration, poly(pyrrole) was synthesized using $LiClO_4$ in different concentrations ranging from 1 mM to 1 M while keeping the pyrrole concentration fixed (0.1 M). The same thing was done with pyrrole concentrations between 1 mM and 1 M (1 M $LiClO_4$ in H_2O). The solvent used was distilled water and the potential for potentiostatic polymerization was 800 mV vs. Ag/AgCl. The samples were characterized by conductivity measurements in the same manner as in part 1 of this series.

AFM pictures were taken using a Digital Instruments Nanoscope III scanning probe microscope run in AFM tapping mode.

RESULTS AND DISCUSSION

The fibre conductivity as a function of monomer and salt concentration in the bulk is shown in *Figure 5*. The conductivities were normalized by dividing them by the conductivity at 1 M. As can be seen from the plot, there is a difference in conductivity of two orders of magnitude in going from 1 mM to 1 M in the concentration of monomer in the solution. The influence of the salt concentration follows the well-established behaviour, reaching a plateau value around 0.1 M[14,15]. The influence of the monomer concentration can be evaluated using equation (11), since the current density is easily measured during the polymerization. As can be seen from *Figure 4*, the time to reach total coverage of the diffusion zones is very short (within seconds for all different pore sizes), and equation (11) can be simplified to

$$j = nF(c^{b} - c^{m})\sqrt{\frac{D}{\pi t}} \tag{12}$$

when choosing an appropriate time to measure the current. *Figure 6* shows an example of the validity of this expression and the time interval for which the assumptions leading to equations (7) and (12) hold. In *Figure 6*, the bulk concentration of monomer c^{b} is 0.01 M and the time interval for which equation (12) is valid is from 5 to

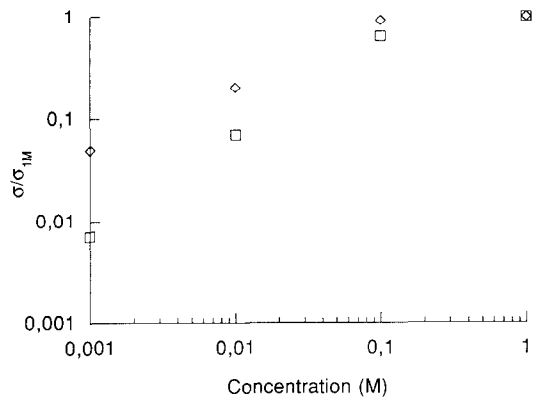

Figure 5 Normalized fibre conductivity as a function of monomer and salt concentration. For the different monomer concentrations (□), the salt concentration was 1 M, and for the different salt concentrations (◇), the monomer concentration was 0.1 M

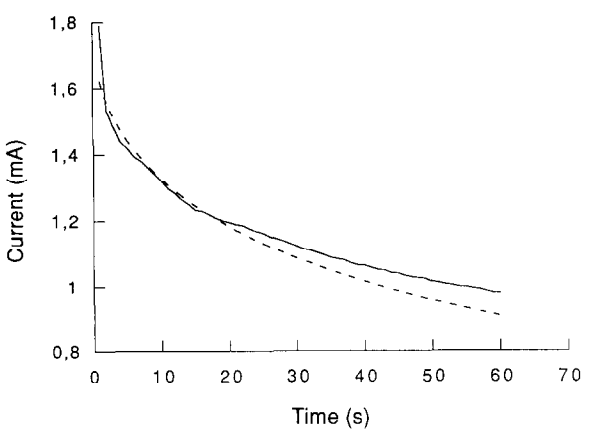

Figure 6 Experimental (solid) and theoretical (dashed) curves for the change in polymerization current with time

Table 3 Calculated values of c^{m}

c^{b} (M)	j (mA cm^{-2})	t (s)	c^{m} (M)
1	30	5	0.724
0.1	4.7	10	0.0728
0.01	0.51	20	0.005 84
0.001	0.031	60	5.62×10^{-4}

Table 4 Values of c^{m} and c^{e} for different bulk concentrations of pyrrole (pore size 100 nm)

c^{b} (M)	c^{m} (M)	c^{e} (M)
1	0.724	0.481
0.1	0.0728	0.0452
0.01	0.005 84	0.001 36
0.001	5.62×10^{-4}	1.08×10^{-4}

Table 5 Values of c^{m} and c^{e} for different pore sizes (bulk concentration of pyrrole 0.1 M)

Pore size (μm)	c^{m} (M)	c^{e} (M)
10	0.059	0.003 47
1	0.063	0.0186
0.1	0.073	0.0452
0.01	0.098	0.0808

20 s. Equation (12) can be rewritten to give an expression for the concentration at the mouth of the pores

$$c^{m} = c^{b} - \frac{j}{nF}\sqrt{\frac{\pi t}{D}} \tag{13}$$

The results from the experiments with different monomer concentrations are summarized in *Table 3*. Knowing c^{m} and assuming a linear diffusion in the pores, the concentration of neutral monomers in the vicinity of the electrode surface c^{e} can be calculated using

$$j_{pore} = nF\frac{D}{L}(c^{m} - c^{e}) \Rightarrow$$
$$c^{e} = c^{m} - \frac{j_{pore}L}{nFD} \tag{14}$$

Using equation (14), the results will be shown in *Table 4*.

In part 1 of this series it was shown that the conductivity is strongly dependent on the pore size. A similar calculation as above has been performed for this case, changing pore size instead of monomer concentration, giving the results shown in *Table 5*. Since the concentration of neutral monomers close to the growing polymer surface can be calculated, another value of interest is the concentration of radicals in the vicinity of this surface. A value that can be readily measured is the current density in the pores j_{pore} (calculated as the measured current density divided by the porosity of the membrane). From j_{pore} a value proportional to the concentration of radicals, a concentration estimate γ, can be calculated using

$$\gamma = \frac{j_{pore}\Delta t}{F\sqrt{D\Delta t}} \tag{15}$$
$$c^{e}_{rad} \propto \gamma$$

where $\Delta t = 30\,\mu$s (according to Raymond and Harrison[16]) is the lifetime of the radical and $\sqrt{D\Delta t}$ is the

Table 6 Values of c^e/γ compared to the conductivity for different bulk concentrations and pore sizes

Pore size (μm)	c^b (M)	c^e/γ	σ_{pore} (S cm^{-1})
0.1	1	29.8	545
0.1	0.1	17.8	349
0.1	0.01	3.26	38.4
0.1	0.001	2.59	3.90
10	0.1	1.16	17
1	0.1	6.85	85
0.1	0.1	17.7	349
0.01	0.1	80.2	1097

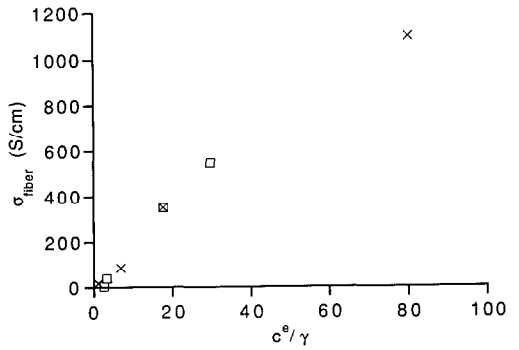

Figure 7 Relationships between fibre conductivity and the ratio c^e/γ for different pore sizes (□) and different monomer concentrations (×)

distance it can travel during its lifetime. The diffusion coefficients are assumed to be equal for neutral monomers and radicals.

A characteristic value for each concentration and pore size would then be the ratio c^e/γ, as this would give an indication of the differences in the polymerization conditions. Values of this ratio, together with the conductivities of the polymer fibre, are given in *Table 6*. The results from *Table 6* are plotted in *Figure 7*. As can be seen from this figure, there is an almost linear relationship between the ratio of neutral monomers and radicals and the resulting conductivity of the polymer fibres. The relationship is consistent both for different monomer concentrations and different pore sizes, and implies that the concentration of radicals should be kept low compared to the concentration of neutral monomers in order to obtain a material with high conductivity. This is in agreement with results from West *et al.*[17], who have shown from electrochemical and optical measurements that poly(pyrrole) grown at low current densities has a higher degree of conjugation. Additional measurements[18] on these low current density films show that they behave in a similar way to poly(pyrrole) in the smaller pores by having higher conductivities and increased ordering compared to normal poly(pyrrole).

To find the underlying reasons for this behaviour is a difficult task. As has been pointed out by a great number of authors, the mechanism of electropolymerization is far from being understood[19,20], and different reactions occur simultaneously in the electrochemical cell[21]. As a result of this, many different factors such as temperature[14,22], concentration[15,23], pH[24], counterion[25], programmed potential[26] and surface pretreatment[27] have been investigated in the search for an optimal electropolymerization method. The results from the present work show that it might be necessary to broaden the perspectives regarding the polymerization mechanism. In the most generally accepted model, at least for poly(pyrrole), it is assumed that the polymerization occurs via radical–radical coupling steps[28]. For most polymerization conditions, there exist experimental and theoretical results that favour this mechanism[20], but deviations have also been found[21,29]. An alternative mechanism would be coupling between a radical and a neutral monomer[29] instead of radical–radical couplings. What we suggest is that both processes could occur, and that the radical–radical coupling is dominant for the current densities used in most polymerization experiments. When the concentration of available radicals decreases, the radical–neutral coupling becomes more and more favoured and the polymerization route is gradually changed, apparently resulting in a more regular polymer. Similar behaviour has been shown for chemical polymerization by Andersson *et al.*[30] in making highly regular poly[3-(4-octylphenyl)thiophene] by keeping the amount of reagent low during the polymerization.

CONCLUSIONS

It has been shown that the increase in conductivity can be regarded as being a result of the polymerization conditions in the pores, where the concentration of radicals is lower than the concentration of neutral monomers in contrast to the case of bulk polymerization. The relationship is close to linear between the fibre conductivity and the ratio c^e/γ for the range of concentrations and pore sizes involved in this investigation. It is proposed that the low concentration of radicals favours a different polymerization route, with radical–neutral coupling instead of radical–radical coupling, resulting in a material with higher regularity.

REFERENCES

1 Calahane, W. and Labes, M. M. *Chem. Mater.* 1989, **1,** 519
2 Cai, Z. and Martin, C. R. *J. Am. Chem. Soc.* 1989, **111,** 4138
3 Granström, M. and Inganäs, O. *Synth. Met.* 1993, **55–57,** 460
4 Liang, W. and Martin, C. R. *J. Am. Chem. Soc.* 1990, **112,** 9666
5 Parthasarathy, R. V. and Martin, C. R. *Chem. Mater.* 1994, **6,** 1627
6 Aoki, K. *Electroanalysis* 1993, **5,** 627
7 Bond, A. M., Luscombe, D., Oldham, K. B. and Zoski, C. G. *J. Electroanal. Chem.* 1988, **249,** 1
8 Spanier, J. and Oldham, K. B. 'An Atlas of Functions', Hemisphere, New York, 1987
9 Diaz, A. F. and Bargon, J. in 'Handbook of Conducting Polymers' (Ed. T. A. Skotheim), Vol. 1, Marcel Dekker, New York, 1986, p. 81
10 Scharifker, B. R. *J. Electroanal. Chem.* 1988, **240,** 61
11 Gunawardena, G., Hills, G., Montenegro, I. and Scharifker, B. *J. Electroanal. Chem.* 1982, **138,** 225
12 Scharifker, B. *Acta Cient. Venez.* 1984, **35,** 211
13 Avrami, M. *J. Chem. Phys.* 1939, **7,** 1103
14 Maddison, D. S. and Unsworth, J. *Synth. Met.* 1989, **30,** 47
15 Satoh, M., Kaneto, K. and Yoshino, K. *Synth. Met.* 1986, **14,** 289
16 Raymond, D. E. and Harrison, D. J. *J. Electroanal. Chem.* 1993, **361,** 65
17 West, K., Jacobsen, T., Zachau-Christiansen, B., Careem, M. A. and Skaarup, S. *Synth. Met.* 1993, **55–57,** 1412
18 Dyreklev, P., Granström, M., Skaarup, S. and Inganäs, O. unpublished results
19 Mitchell, G. R. and Geri, A. *J. Phys. D: Appl. Phys.* 1987, **20,** 1346

20 Heinze, J. *Synth. Met.* 1991, **41–43,** 2805
21 Otero, T. F. and Rodriguez, J. *Electrochim. Acta* 1994, **39,** 245
22 Liang, W., Lei, J. and Martin, C. R. *Synth. Met.* 1992, **52,** 227
23 Lei, J., Cai, Z. and Martin, C. R. *Synth. Met.* 1992, **46,** 53
24 Kupila, E.-L. and Kankare, J. *Synth. Met.* 1993, **55–57,** 1402
25 Hyodo, K. and MacDiarmid, A. G. *Synth. Met.* 1985, **11,** 167
26 Kiani, M. S., Bhat, N. V., Davis, F. J. and Mitchell, G. R. *Polymer* 1992, **33,** 4113
27 Kupila, E.-L. and Kankare, J. *Synth. Met.* 1994, **62,** 55
28 Genies, E. M., Bidan, G. and Bidan, A. F. *J. Electroanal. Chem.* 1983, **149,** 101
29 Asavapiriyanont, S., Chandler, G. K., Gunawardena, G. A. and Pletcher, D. *J. Electroanal. Chem.* 1984, **177,** 229
30 Andersson, M. R., Selse, D., Järvinen, H., Hjertberg, T., Inganäs, O., Wennerström, O. and Österholm, J.-E. *Macromolecules* 1994, **27,** 6503